Atmospheric Pollution Research 13 (2022) 101452

Contents lists available at ScienceDirect

Atmospheric Pollution Research

journal homepage: www.elsevier.com/locate/apr

Meteorology-normalized variations of air quality during the COVID-19 lockdown in three Chinese megacities

Yunqian Lv [a,b], Hezhong Tian [a,b,*], Lining Luo [a,b], Shuhan Liu [a,b], Xiaoxuan Bai [a,b], Hongyan Zhao [a,b], Shumin Lin [a,b], Shuang Zhao [a,b], Zhihui Guo [a,b], Yifei Xiao [a,b], Junqi Yang [a,b]

[a] State Key Joint Laboratory of Environmental Simulation & Pollution Control, School of Environment, Beijing Normal University, Beijing, 100875, China
[b] Center for Atmospheric Environmental Studies, Beijing Normal University, Beijing, 100875, China

ARTICLE INFO

Keywords:
COVID-19
Air quality
Random forest model
Meteorological impacts
Road traffic
Emission control strategy

ABSTRACT

To avoid the spread of COVID-19, China implemented strict prevention and control measures, resulting in dramatic variations in air quality. Here, we applied a machine learning algorithm (random forest model) to eliminate meteorological effects and characterize the high-resolution variation characteristics of air quality induced by COVID-19 in Beijing, Wuhan, and Urumqi. Our RF model estimates showed that the highest decrease in deweathered $PM_{2.5}$ in Wuhan (−43.6%) and Beijing (−14.0%) was at traffic stations during lockdown period (February 1- March 15, 2020), while it was at industry stations in Urumqi (−54.2%). Deweathered NO_2 decreased significantly in each city (~30%–50%), whereas accompanied by a notable increase in O_3. The diurnal patterns show that the morning peaks of traffic-related NO_2 and CO almost disappeared. Additionally, our results suggested that meteorological effects offset some of the reduction in pollutant concentrations. Adverse meteorological conditions played a leading role in the variation in $PM_{2.5}$ concentration in Beijing, which contributed to +33.5%. The true effect of lockdown reduced the $PM_{2.5}$ concentrations in Wuhan, Beijing, and Urumqi by approximately 14.6%, 17.0%, and 34.0%, respectively. In summary, lockdown is the most important driver of the decline in pollutant concentrations, but the reduction of SO_2 and CO is limited and they are mainly influenced by changing trends. This study provides insights into quantifying variations in air quality due to the lockdown by considering meteorological variability, which varies greatly from city to city, and provides a reference for changes in city scale pollutant concentrations during the lockdown.

1. Introduction

Air pollution is a global public health concern, particularly in developing countries such as China (Lelieveld et al., 2015) and India (Guo et al., 2017). In 2015, $PM_{2.5}$ pollution was responsible for 4.2 million deaths a year globally, including 1.1 million in China (Cohen et al., 2017). Studies have shown that poor air quality increases the prevalence and mortality of novel coronavirus pneumonia (Coccia, 2020; Liang et al., 2020).

To prevent the spread of COVID-19, governments throughout the world have imposed strict lockdown measures (Tian et al., 2020), which have led to a visible decline in economic activity and thus reduce air pollutant emissions (Le et al., 2020). The unprecedented decline in human activities caused by the COVID-19 lockdown provides a unique natural-triggered experimental chance to research the possible impacts of anthropogenic emissions on air quality and a basic reference for promulgating air pollution management regulations in the coming years.

Many studies have analyzed air quality variations due to COVID-19. Most of them compared observed air pollutants during the lockdown with before the lockdown or historical periods through satellite remote sensing (Liu et al., 2020a) or ground observations (Mahato et al., 2020). Several studies even compared changes in pollutants under similar weather conditions (Collivignarelli et al., 2020). However, the concentration variations in various air pollutants are determined jointly by meteorological factors and emissions (Cameletti, 2020). Additionally, numerous actions have been implemented to alleviate atmospheric pollution over the years (Zhang et al., 2019). Furthermore, changes in

Peer review under responsibility of Turkish National Committee for Air Pollution Research and Control.
* Corresponding author. State Key Joint Laboratory of Environmental Simulation & Pollution Control, School of Environment, Beijing Normal University, Beijing, 100875, China.
E-mail address: hztian@bnu.edu.cn (H. Tian).

https://doi.org/10.1016/j.apr.2022.101452
Received 21 December 2021; Received in revised form 7 May 2022; Accepted 7 May 2022
Available online 14 May 2022
1309-1042/© 2022 Turkish National Committee for Air Pollution Research and Control. Production and hosting by Elsevier B.V. All rights reserved.

the heating season are also one influencing factor. Therefore, it is inaccurate to simply compare the observed values of pollutant concentrations before and after the lockdown. Comparisons between 2019 and other years (e.g., the average value from 2015 to 2017) are also likely to be skewed. These results may not be sufficient to reveal the impact of emissions control measures and changes in meteorological conditions. A series of studies used chemical transport models to assume reductions in emissions (Wang et al., 2020) and estimate the impact on pollutant concentrations (Liu et al., 2020b). However, it is difficult to estimate emission changes attributed to the lockdown.

Several studies have applied mathematical models to evaluate the impact on air quality. Venter et al. (2020) used the multiple linear regression model to make predictions in 34 various countries in the world. Bao and Zhang (2020) used the least square dummy variable model (LSDV model) to investigate variations in northern China. Wang et al. (2021) established one difference-in-difference model to evaluate the impact in the Beijing-Tianjin-Hebei region. In addition, the impact of travel bans and the strength of regulatory behavior on air quality heterogeneity were also discussed. However, the accuracy of the adopted model is relatively low, e.g., the model accuracy of Venter et al. (2020) is usually less than 0.6, and some assumptions applied in the model are also uncertain.

As a reliable method, machine learning can be used to quantify changes in air quality caused by meteorology and emissions. In fact, several studies have applied the RF (random forest) model to remove the impact of meteorology. Vu et al. (2019) used the RF model to normalize the meteorology of six criteria pollutants in Beijing from 2013 to 2017, to evaluate the effectiveness of the clean action plan in reducing the level of air pollution in Beijing. Petetin et al. (2020) used the ML model to investigate the reduction in NO_2 concentration in Spain due to the COVID-19 lockdown and found that NO_2 mixing ratios at urban background and traffic stations were found to decrease by approximately −50% due to the lockdown. Cole et al. (2020) used the RF method to eliminate the mixed influence of meteorological conditions. They found that NO_2 concentrations fell by as much as 24 $\mu g/m^3$ during the lockdown while there was no obvious change trend of SO_2 and CO.

Previous studies have been performed to analyze air quality variations related to COVID-19. However, few of them take into account the detailed studies of all 6 criteria air pollutants at different types of monitoring stations. Additionally, there is a lack of investigation on the impact of meteorology on the variations. In addition, the analysis of the high spatial resolution of cities in western China is also lacking. Therefore, in this study, we combined a weather normalization technique optimized by Shi et al. (2021) to provide a comprehensive assessment of the air quality variations induced by COVID-19 at a multiscale (multicity, multistation, multipollutant) and high spatial-temporal resolution, which included Wuhan (located in Central China and breakout epicenter of COVID-19), Beijing (located in North China and the Capital of China) and Urumqi (located in Western China and Capital city of Xinjiang Autonomous Region). Additionally, ground air quality monitoring stations in these cities were divided into four types to examine the influence of emission source changes on ambient air pollution. This study examined the potential causes of changes in pollutant concentrations and provides a reference for the change in pollutant concentrations at the urban scale during the lockdown period. To the best of our knowledge, this is the first study to explore the impact of the COVID-19 pandemic on six different criteria pollutants in eastern, central, and western China with high temporal and spatial resolutions, especially considering meteorological variability.

2. Materials and methods

2.1. Study areas and data sources

2.1.1. Description of study areas

Three cities were selected with different longitudes with strong spatial representation in our study, which were named Beijing, Wuhan, and Urumqi. These three cities were geographically located in eastern, central, and western China, respectively (see Fig. 1). New coronavirus disease first broke out in Wuhan (Li et al., 2020). Beijing and Urumqi have also been affected along with the evolution and diffusion of the COVID-19 pandemic. Additionally, their climatic conditions and air quality are quite different. These cities permitted the study of the heterogeneity of air quality variations related to COVID-19 lockdown in different regions.

2.1.2. Data sources

The hourly data of criteria air pollutants (CAPs, which include NO_2, $PM_{2.5}$, O_3, PM_{10}, SO_2, and CO) were acquired from China National Environmental Monitoring Center (CNEMC). It included data from January 1 to May 31 each year for six years from 2015 to 2020. In Wuhan, data from 9 stations were used. In Beijing, 16 stations were analyzed. In Urumqi, 6 stations were selected (see Fig. 1). Among these stations, they were distinguished into four categories according to the characteristics of the station's surroundings: urban, traffic, industry, and rural stations. For example, the traffic station is determined as a station closer to the heavy traffic hub. Industry stations are defined as many industrial parks nearby, which are more affected by industrial emissions. The detailed classification information was shown in Table S1. The hourly wind speed, wind direction, temperature, relative humidity, and atmospheric pressure for selected cities are obtained using the "worldmet" R software package from the nearest weather station (https://CRAN.R-project.org/package=worldmet). Fig. 1 shows the map of the study areas. Detailed information is summarized in Table S1.

2.2. De-weather model

Changes in the concentrations of atmospheric pollutants are jointly affected by emissions and meteorology. To highlight the role of emissions, the "normalweatherr" R package (Vu et al., 2019) was utilized to eliminate the impact of meteorological factors (Grange and Carslaw, 2019). Here, a machine learning-based RF algorithm optimized by Shi et al. (2021) was applied to eliminate the influence of meteorology.

Random forest (RF) is a statistical learning theory. It uses the bootstrap resampling method to extract multiple samples from the original sample, conducts decision tree modeling for each bootstrap sample, and then combines the prediction of multiple decision trees to obtain the final prediction result through voting. In general, a random forest randomly generates hundreds to thousands of classification trees and then selects the tree with the highest degree of repetition as the final result (Breiman, 2001).

The overall idea of the RF algorithm includes first predicting the concentration of pollutants based on a set of characteristic values (including meteorological data and other time variables) and training a reliable RF model. Then, the RF model can be used to predict the concentration of pollutants under a series of meteorological conditions, and the relevant average value is called the normalized time series of meteorology. In the algorithm, the concentration of a certain pollutant at a specific time point can be predicted by resampling meteorological data. This process was repeated 1000 times, and 1000 predicted concentrations were averaged to calculate the final weather standardized concentration for that particular hour, day, and year. In the process, only the weather data, not the time variable, was normalized and resampled from the entire study period. The flowchart of the machine learning-based RF algorithm can be observed in Fig. ST1.

In this study, RF models were developed for each pollutant at each monitoring station for the corresponding period each year (January to May of each year from 2015 to 2020). The air pollutant concentration predicted by the RF model was the meteorological normalized concentration (called the "deweathered" concentration). The weather normalization was carried out by the "rmweather" R package. Details of the models can be observed in the separate Supporting Information (SI)

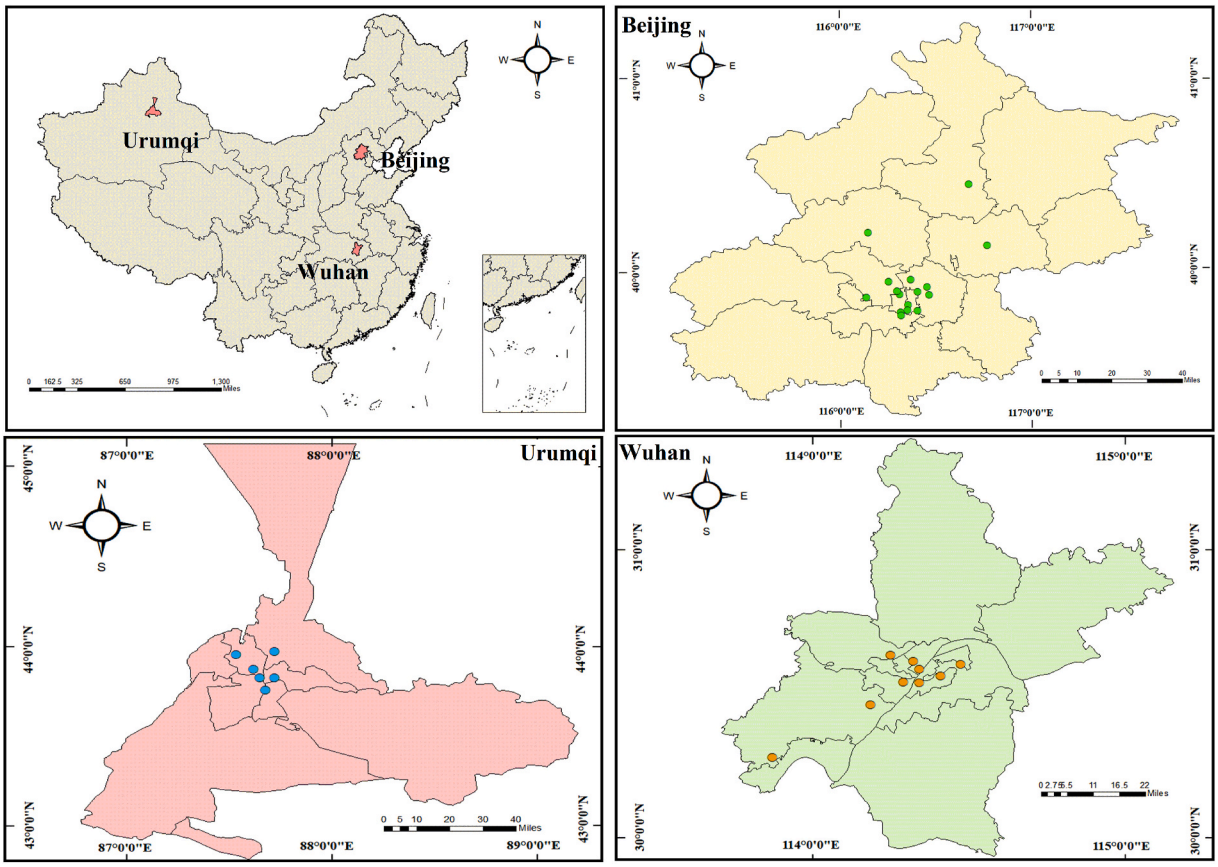


Fig. 1. Map of the study areas (The circles point out the location of air quality monitoring stations).

provided with this study.

2.3. Data analysis

For better analysis, the study time span spilled two periods: pre-lockdown period (before the lockdown: January 1–20, "PD") and lockdown period (during the lockdown: February 1- March 15, "LD"). First, the percentage change in observed pollutant concentrations (P_{obs}) was calculated by comparing the observed concentration between PD and LD in 2020. To exclude the effect of meteorological conditions and reveal the variations in emissions. The changes in deweathered concentrations (P_{dew}) were calculated by the relative changes in deweathered pollutant concentrations in PD and LD. The difference between P_{obs} and P_{dew} indicated the contribution of meteorology to the changes in the pollutant concentration observations. Furthermore, the historical data for 2015–2019 during the same time span were a criterion for detrending. The average percentage change in pollutant concentration between PD and LD from 2015 to 2019 was taken as the "trend" item to represent the change in emissions when "business as usual". Additionally, the moving average of deweathered concentrations was calculated from 2015 to 2019 as the baseline to eliminate meteorological effects as much as possible. Finally, the detrended variation rate (P*) was calculate dby Eq. (1):

$$P^* = P_{2020} - P_{2015\text{-}2019} \quad (1)$$

where P_{2020} and $P_{2015–2019}$ represent the deweathered concentration variation rates (LD versus PD) in 2020 and 2015–2019, respectively. P* reflected the extent to which air quality was truly affected by the lockdown.

3. Results and discussion

3.1. Evaluation of model performance

Ten statistical indices were used to evaluate our model in different ways. The model evaluation metrics are shown in Table 1. The high R values range 0.81–0.94 indicate that the relation between the predicted values and the observed values was significant. The RF model performance is shown in Fig. 2. The R^2 values were generally higher than 0.6, and some were even higher than 0.9. This indicates that the features of the established model were excellent and far better than those of the regression model (Venter et al., 2020). FAC2 values of 0.92, 0.91, 0.94, 0.93, 0.98, and 0.90 for $PM_{2.5}$, PM_{10}, NO_2, SO_2, CO, and O_3, which suggest that our model satisfies the condition for the fraction of predictions. MB value ranged −0.15-0.12 show that the bias produced by our model was very small. Similarly, the lower values of NMB and NMGE indicate that our model performed well. It was considered that our model had satisfactory prediction capability, as verified by all the indices.

3.2. Diurnal variations in air pollutants

The diurnal variation in pollutant concentration is closely related to the trajectory of human activities. A change in anthropogenic emissions has an important impact on the variations in air pollutant concentrations at different times in a day. Therefore, in this section, the diurnal variations in CAPs during the lockdown are examined, which provides insight into the interrelationship between air pollutants and different emission sources.

The diurnal variations in pollutants at four types of stations in three cities can be observed in Fig. 3 and S1. NO_2 and CO are air pollutants related to traffic activities with a bimodal distribution at each traffic

Table 1
RF model performance for testing data set (in hourly time resolution).

Pollutants	RMSE	R	R^2	FAC2	MB	MGE	NMB	NMGE	COE	IOA
$PM_{2.5}$	19.8	0.94	0.86	0.92	0.12	12.45	0.00	0.20	0.68	0.84
PM_{10}	42.2	0.87	0.79	0.91	0.11	23.60	0.00	0.24	0.58	0.79
NO_2	13.6	0.88	0.75	0.94	0.06	9.64	0.00	0.22	0.57	0.79
SO_2	6.7	0.81	0.70	0.93	−0.05	3.01	−0.00	0.25	0.56	0.78
CO	0.3	0.87	0.71	0.98	0.004	0.19	0.01	0.17	0.62	0.81
O_3	13.4	0.94	0.88	0.90	0.07	9.40	0.00	0.17	0.71	0.85

Note: FAC2 (fraction of predictions with a factor of two), MB (mean bias), MGE (mean gross error), NMB (normalized mean bias), NMGE (normalized mean gross error), COE (Coefficient of Efficiency), IOA (Index of Agreement).

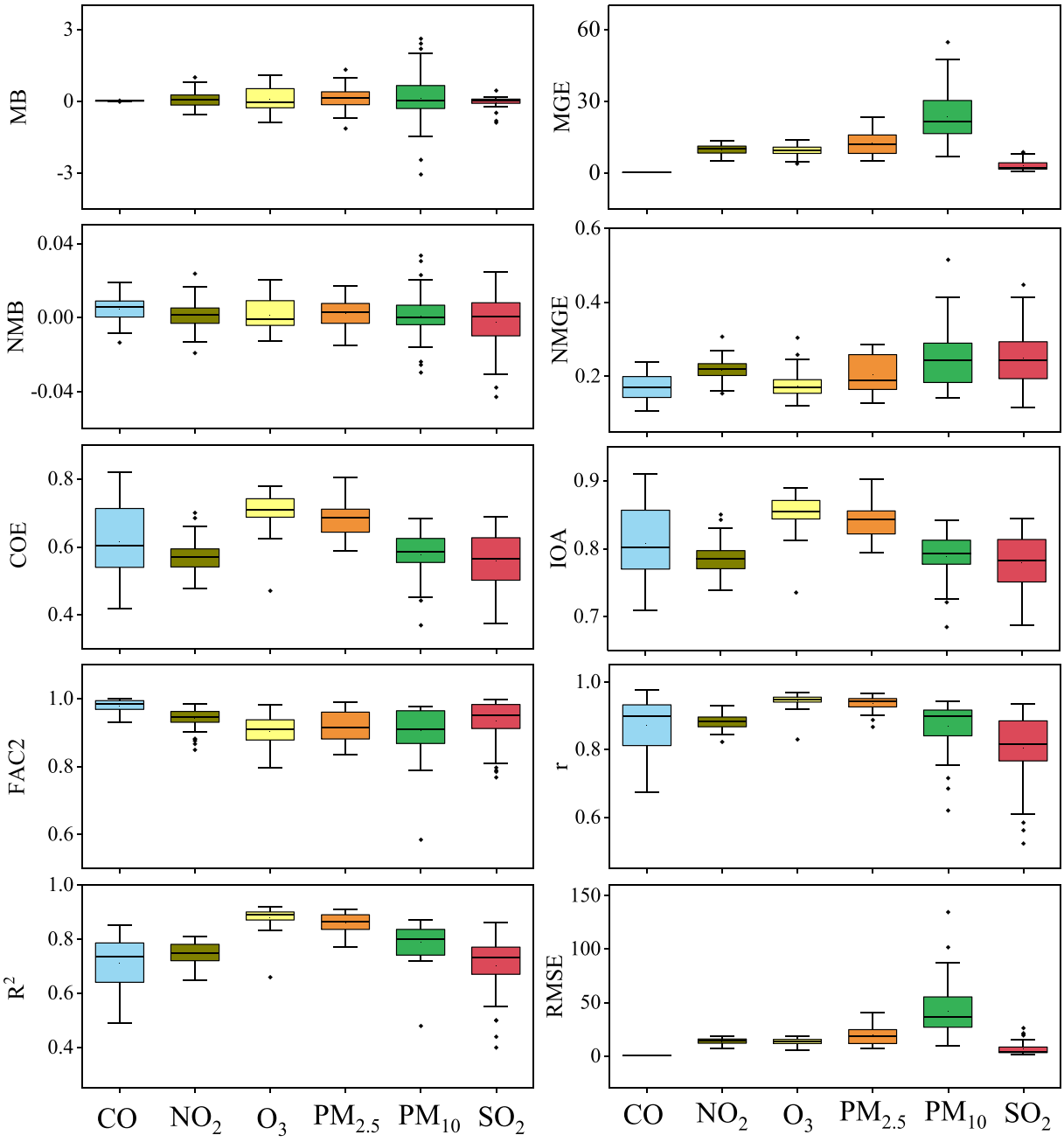


Fig. 2. Model validation for testing data set of each air pollutant (in hourly time resolution) in 2015–2020.

station. Fig. 3a shows that double peaks occurred at 8:00–9:00 and 20:00–21:00 in Beijing and Wuhan but approximately 2 h later in Urumqi, which can be explained by the time difference of a 2-h lag between Urumqi and Beijing (Beijing Time is adopted in all of China). Similar to other studies, the peak distribution of the diurnal variations of ambient NO_2 and CO was closely related to the commuting peak time at local (Singh et al., 2020; Sheng et al., 2019). At urban and traffic stations, traffic is the leading source of CO. With the decrease in traffic

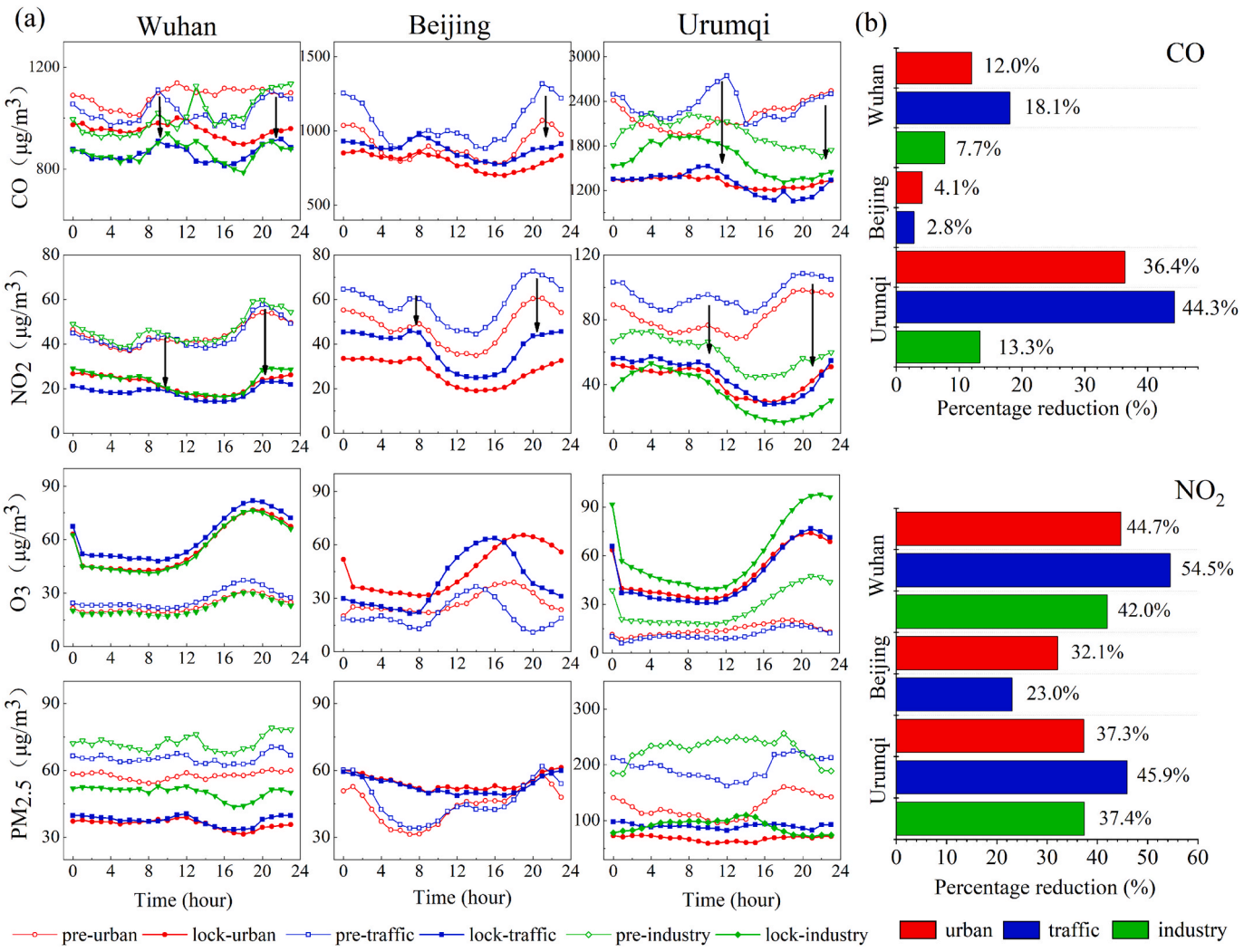


Fig. 3. (a) Diurnal concentration variations of CO, NO_2, O_3, and $PM_{2.5}$ pollutants at three types of stations in three cities during lockdown period (1 February to 15 March) versus pre-lockdown period (1 January to 20 January). (b) Percentage reduction in morning peak of CO and NO_2 during the lockdown.

flow, CO peak weakened significantly at urban stations and traffic stations, especially at traffic stations (see Fig. 3a), which suggested that the COVID-19 lockdown had a greater impact on CO concentrations at traffic stations. However, the source of CO at the industry station was mainly from industrial activities, and the industrial activities were less interrupted during the lockdown. Therefore, the decline of CO peak at industry stations (−7.7% in Wuhan and −13.3% in Urumqi, see Fig. 3b) is much smaller than that at urban and traffic stations.

On lockdown days, the daily cycle variation pattern of NO_2 at all types of monitoring stations was similar (Fig. 3a and S1). In summary, although the peak value of NO_2 was weak in lockdown, the daily cycle variation trend of its production and depletion was the same as that before the lockdown, suggesting the inherent diurnal photochemical reaction cycle of NO_2. Compared with CO, a larger decline in the peak value of NO_2 was observed (see Fig. 3b), showing a closer relationship between traffic activities, which is consistent with previous studies (Venter et al., 2020; Wang et al., 2020). The peak concentration of NO_2 related to morning and evening traffic activities decreased markedly, which coincides with the substantial decline of public travel patterns on working and schooling from home during the pandemic owing to lockdown and quarantine policies. Similar to CO, the decrease in the peak value at traffic stations was the most marked (Fig. 3a). As illustrated in Fig. 3b, the morning peak value of NO_2 in Wuhan, Beijing, and Urumqi decreased by 54.5%, 23.0%, and 45.9%, respectively, coinciding with the noticeable reduction in traffic volumes.

As an important precursor for O_3 production, NO_2 has an important influence on the daily variations in O_3. The O_3 concentration peaked in the late afternoon hours in Wuhan and Beijing and much later in Urumqi because of the long daylight hours. In Beijing, different daily circulation patterns between traffic and non-traffic stations were observed (Fig. 3a). The O_3 peak of traffic stations was about 3 h earlier than at non-traffic stations, revealing the important contribution from the exhaust of vehicles. During the lockdown, the O_3 concentration unexpectedly increased, especially at traffic stations, where there was a sharper increase at the peak, which may be caused by a decrease in the titration reaction. Additionally, O_3 peaked slightly later in the lockdown period. A higher increase in O_3 concentrations at night than during the day was observed (Fig. 3a).

$PM_{2.5}$ comes from complex sources and the generation of secondary aerosols is affected by a variety of factors. The general diurnal variation showed a bimodal distribution at most stations but was not evident (Fig. 3a and S1). The peak in the morning was due to traffic emissions, while the increase in the evening was closely related to household emissions (Srivastava et al., 2021). Before the lockdown, the diurnal variation pattern of PM at each station was inconsistent, but after the lockdown, the daily variation trend in PM at all stations in each city was similar and the average daily variation range was small, perhaps related to the reduction in human activities.

Overall, although air pollutant concentrations responded to changes in variations in emission sources, peak times did not change significantly, which indicates that meteorology acted a major characteristic in CAP variations compared with reductions in anthropogenic emissions.

3.3. Concentration variations due to activity changes after excluding the meteorological impact

The observed NO_2 levels were highly variable, with daily concentrations changing notably during the study period (Fig. 4 and S2). The mean levels of NO_2 declined by 49.7%, 42.9%, and 48.1% during the lockdown in Wuhan, Beijing, and Urumqi at urban stations, respectively (Table S2). At traffic stations, the reduction percentage of observed NO_2 ranged from 33.5% to 57.7%. At the same time, observed NO_2 at industry stations and rural stations also decreased significantly after the lockdown (Fig. S2).

Deweathered NO_2 exhibits a similar pattern to that of the observed value, but the magnitude of the change is different. A sudden decrease in deweathered NO_2 during the lockdown period was observed in Wuhan and Urumqi, but not pronounced in Beijing (Fig. 4), which is consistent with previous studies (Wu et al., 2021). This may be related to the fact that Beijing still has a high level of necessary traffic activity during the epidemic (Fig. S7). Fig. S7 shows that the Travel Intensity of Wuhan and Urumqi has dropped to the extreme, while Beijing has an obvious weekend effect. Meanwhile, the timing of the rapid decline for deweathered NO_2 was remarkably coincident with the start of the lockdown in Wuhan. However, a few days after the lockdowns, there was a sudden drop in Urumqi. This may be because of undemanding control measurements at the beginning in Urumqi. The change percentages of deweathered NO_2 at urban stations in Beijing, Urumqi, and Wuhan were −32.2%, −34.8%, and −43.7%, respectively (Table 2). Deweathered NO_2 decreased the most in Wuhan because of the stringent lockdown measures. A sudden drop, distinct from the data in 2019, is clearly observed in 2020 after the lockdowns began, especially in Urumqi (Fig. 4 and S2). This confirms that the sudden decline in 2020 was caused by the lockdown measures.

In contrast to changes in NO_2, observed O_3 follows an increasing trend during the lockdown at all stations (Fig. 4 and S2). Because of the weakening of unbalanced economic activity, the decline in NOx emissions of the study cities is greater than that of VOC emissions, resulting in a decrease in the titration effect to O_3. In addition, the decrease in PM concentration will also result in increased O_3 concentrations (Liu et al., 2013). Due to the low PM emissions in the lockdown period, higher insolation also promotes the formation of O_3 (Murphy et al., 2007). Observed O_3 in Urumqi increased the most, with the percentage changes ranging from +54.5% in Beijing to +243.0% in Urumqi (Table S2). In contrast to observations, deweathered O_3 increased the most in Wuhan because automobile exhaust contributes the most to O_3 production, contributing 30% on days when O_3 is not high (Zeng et al., 2018). The minimum increment of deweathered O_3 during the lockdown period is

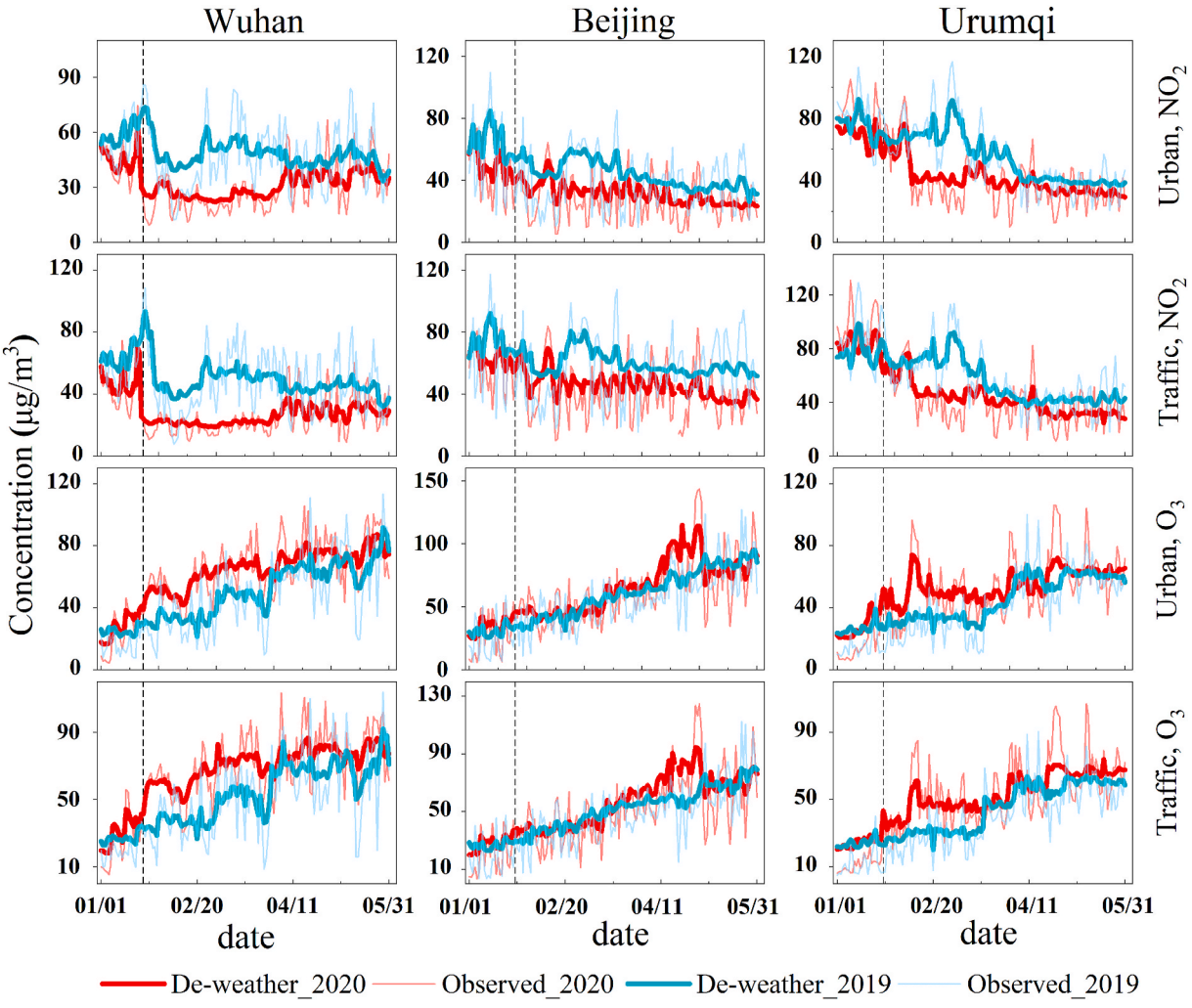


Fig. 4. Daily average concentration of observed and deweathered NO_2 and O_3 at urban and traffic stations in three cities from 1 January to 31 May in 2020 versus 2019.

Table 2
Change rates (%) in deweathered and detrended mass concentrations of CAP at urban stations and traffic stations during the study period (2020.2.1–3.15 vs 2020.1.1–1.20) in the three studied cities.

	Deweathered	NO_2	O_3	$PM_{2.5}$	PM_{10}	CO	SO_2
Wuhan	urban	−43.7%	+115.3%	−36.9%	−30.6%	−11.5%	+1.0%
	traffic	−55.2%	+114.3%	−43.6%	−30.2%	−15.6%	−5.3%
Beijing	urban	−32.2%	+39.6%	−11.8%	−3.1%	−31.2%	−29.4%
	traffic	−24.8%	+49.7%	−14.0%	−5.1%	−34.3%	−25.5%
Urumqi	urban	−34.8%	+93.0%	−45.3%	−14.5%	−32.3%	+2.3%
	traffic	−39.1%	+93.3%	−50.3%	−27.0%	−33.0%	−7.8%
	Detrended	**NO_2**	**O_3**	**$PM_{2.5}$**	**PM_{10}**	**CO**	**SO_2**
Wuhan	urban	−33.2%	+69.3%	−14.6%	−17.3%	−3.6%	+18.6%
	traffic	−46.2%	+57.3%	−21.7%	−19.9%	−2.8%	+8.3%
Beijing	urban	−19.8%	+2.1%	−17.0%	+6.0%	−12.2%	−9.1%
	traffic	−16.4%	+7.0%	−16.6%	+2.9%	−16.0%	−7.2%
Urumqi	urban	−31.8%	+40.1%	−34.0%	−8.7%	−16.7%	+13.7%
	traffic	−25.3%	+35.4%	−34.7%	−20.0%	−15.2%	+3.6%

observed in Beijing. The percent change for deweathered O_3 ranged from +49.7% in Beijing to +114.3% in Wuhan at traffic stations, from +39.6% in Beijing to +115.3% in Wuhan at urban stations, and from +32.4% in Beijing to +68.4% in Wuhan at rural stations, respectively (Table S3). The smallest increase at rural stations was observed among the four types of stations in all three cities. Increased O_3 concentrations are also found in other cities across the world, including Delhi (Sharma et al., 2020; Rathod et al., 2021), the Yangtze River Delta (Yuan et al., 2021), and Nice (Sicard et al., 2020). These studies reveal that coordinated NO_2 and VOC control is required to restrain urban and regional ground-level O_3 pollution.

As shown in Fig. 5, during the lockdown, observed $PM_{2.5}$ dropped most significantly in Urumqi, where air pollution was more severe in winter, and no distinct change was observed in Wuhan and Beijing. To one's surprise, in Beijing and Urumqi, pollution incidents still occurred during the lockdown (Fig. 5). During the study period, average observed $PM_{2.5}$ concentrations at urban stations in Wuhan, Urumqi, and Beijing were 36.4 ± 17.6 μg/m^3, 67.9 ± 53.0 μg/m^3, 53.5 ± 53.2 μg/m^3, respectively, which decreased 36.7%, 45.6% and increased 21.7% (see Table S2), respectively.

Compared with the large variation range of observed values, deweathered $PM_{2.5}$ had a clearer trend and pattern than observed $PM_{2.5}$, especially in Beijing (Fig. 5). The $PM_{2.5}$ concentrations in the lockdown period were lower and less variable. Unlike deweathered NO_2, no abrupt drop in deweathered $PM_{2.5}$ was observed after lockdown started in Beijing, Wuhan, and Urumqi. However, it can be seen from Fig. 5 that



Fig. 5. Observed and deweathered daily $PM_{2.5}$ concentrations at four types of stations in three cities from 1 January to 31 May in 2020 versus 2019.

sudden decreases were observed in Wuhan and Urumqi a few days after the lockdown began but less so in Beijing. After the first week of the lockdown, people were able to use private cars despite the disruption to public transport in Wuhan and traffic with other cities (Pei et al., 2020). In Beijing, there was an increase in deweathered $PM_{2.5}$ after the lockdown began initially, but there was a decrease afterward.

During our study period, the P_{dew} values (Table 2 and S3) for deweathered $PM_{2.5}$ range from −14.0% in Beijing to −50.3% in Urumqi at traffic stations, from −11.8% in Beijing to −45.3%% in Urumqi at urban stations, and from −33.6% in Wuhan to −54.2% in Urumqi at industry stations. Among Beijing and Wuhan, the largest decrease was found at traffic stations. Generally, the local road traffic sources have been suggested to be the dominate contributor to $PM_{2.5}$ on the road of heavy traffic (Hu et al., 2014). Meanwhlie, a significant decrease in volume of petrol and diesel vehicles was reported during the COVID-19 pandemic (Wang et al., 2020), the average speeds in Beijing increased overall by 43% from January 24 to February 9, and traffic volumes decreased by 58% (Wang et al., 2020). Additionally, the deweathered $PM_{2.5}$ dropped more markedly in Urumqi, especially at the industry station. It reflects the different industrial structures of each city and the different pollution source apportionments. In addition, the lockdown measures have different effects on the production and economic activities in different cities. Both traffic and industrial activity in Urumqi have dropped significantly. Consistent with previous studies, lockdown may have a greater impact on colder and more industrially polluted cities (He et al., 2020). The fact that substantial decreases in $PM_{2.5}$/CO (Fig. S5) and $PM_{2.5}/PM_{10}$ (Fig. S6) ratios in Urumqi accompanied the decrease in deweathered $PM_{2.5}$. Ultrastrict short-term control measures are more effective in alleviating $PM_{2.5}$ pollution in Urumqi.

The overall changes in PM_{10} are larger than those in $PM_{2.5}$, and there is more variability at different stations (Fig. S3). In general, the sudden decline can be observed after the lockdown, but less impact on industry stations. In Beijing, the trend of PM_{10} was similar to that of 2019. In addition, an increase in deweathered PM_{10} at rural stations was observed in Beijing. Compared with Wuhan and Beijing, a clear downward trend was observed in Urumqi (Fig. S3). Deweathered PM_{10} decreased most at the industry station in Urumqi (−38.2%), reflecting the source of industrial dust.

Deweathered CO levels were lower after lockdown started than before in 2020. A sudden change is observed in Urumqi only (Fig. S4). In Beijing, deweathered CO increased slightly after the lockdown began, before falling for about 2 weeks, after which there was a substantial increase at all three types of stations. In Wuhan, the decreasing trend in deweathered CO is not distinguishable from that in 2019. In Urumqi, a decline in deweathered CO is observed a week after the lockdown began, with −32.3% at urban stations and −33.0% at traffic stations. With the economic development, the number of motor vehicles in Urumqi has increased rapidly. The restriction of traffic in Urumqi during the COVID-19 lockdowns significantly reduced the concentration of major pollutants in car exhaust in the ambient air. Changes in traffic flow have a great impact on CO concentration in the air.

Deweathered SO_2 decreased from west to east, with higher concentration values (6.9–13.5 μg/m^3) in Urumqi and Wuhan and lower values (4.4–5.6 μg/m^3) in Beijing during lockdown (see Table S3). The variation in deweathered SO_2 relied on specific stations and cities. No sudden change is observed in any of the cities immediately after the lockdowns. In Beijing, deweathered urban and traffic SO_2 increased at first and then decreased by ~30%. In opposite, the increase in deweathered rural SO_2 might be relevant to rising resident combustion. Meanwhile, deweathered SO_2 in 2020 was significantly lower than in 2015–2019, indicating that from 2013 to 2017, a number of SO_2 governance solutions have had a positive effect on reducing SO_2 (Zhang et al., 2019; Xue et al., 2019). Therefore, the reduction in SO_2 is relatively limited. A huge decrease in deweathered SO_2 at industry stations reflects the heavy industry structure of Urumqi.

3.4. Driving forces of variations in air pollutants

3.4.1. The influence of meteorology

In our study, a great difference between observed and deweathered pollutants concentrations can be observed among three cities (Fig. 4 and S2 to S4), reflecting the importance of the meteorological effect. Fig. 6 illustrates the contribution of meteorology and anthropogenic emissions to percentage changes of six pollutants concentrations (2020.2.1–3.15 vs. 2020.1.1–1.20) at urban stations in Beijing, Wuhan, and Urumqi.

Different temporal variations and distinct meteorological and emission impacts could be found among the three cities. Except for O_3, anthropogenic emissions of most pollutants were reduced. In Beijing, observed $PM_{2.5}$ increased by 21.7% (Table S2). However, the increase in $PM_{2.5}$ is mainly due to adverse meteorological conditions, which contributed to +33.5%. The deweathered concentrations of air pollutants were significantly lower than their observed values, indicating unfavorable meteorological conditions for pollutant dispersion (Zhang et al., 2020). In fact, the emission reduction contributed to an 11.8% decrease in $PM_{2.5}$ (Table 2). A credible interpretation for this unexpected outcome was that an increase in secondary aerosol formation counteracts the benefit of the reduction in primary $PM_{2.5}$ emissions (Huang et al., 2021). The fact that great increases in $PM_{2.5}$/CO ratios along with the increase in deweathered $PM_{2.5}$ in Beijing was observed in Fig. S5. Our study demonstrates that meteorology contributes the most to variations in pollutant concentrations in Beijing. The results are similar to those of previous studies (Wang et al., 2020; Li et al., 2020; Sun et al., 2020; Zhao et al., 2021). Therefore, except for strict local emission control from industry, transportation as well as residential use, air pollution control in Beijing should strengthen regional joint prevention and control as well as heavy pollution weather emergency measures.

The effects of O_3 are more complex. In Beijing, observed O_3 increased by 76.4%, with emissions accounting for +39.6% and meteorology accounting for +36.8%. In Urumqi, unfavorable meteorological conditions predominated. In contrast, the level of O_3 in Wuhan significantly increased by 115.3%, primarily due to large changes in precursor

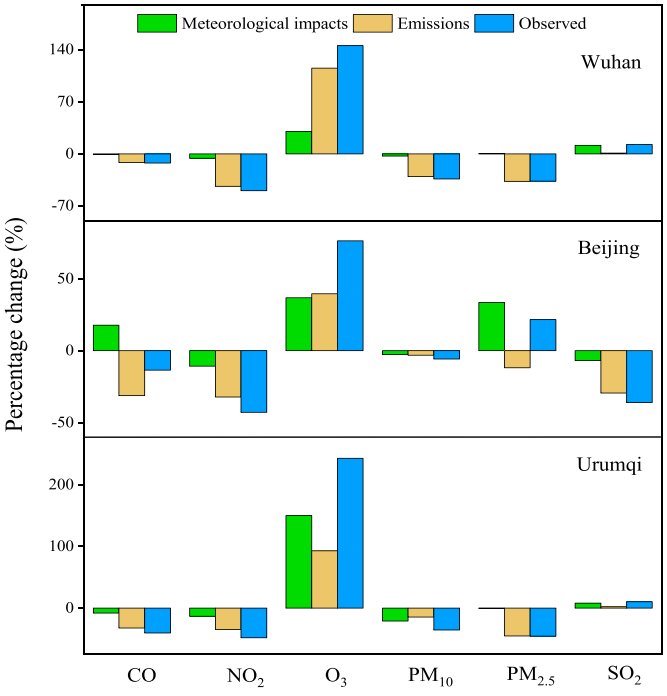


Fig. 6. Proportion of contribution of meteorological and emission factors to the change rate of six pollutants concentrations (2020.2.1–3.15 vs. 2020.1.1–1.20) at urban stations in three cities.

emissions, especially for NO_2. In short, emission variations and meteorology contribute to the increase in ground-level O_3. From this natural experiment, O_3 pollution does not only occur during the hot summer months; reducing NO_x emissions such as this simply is not the right approach (Huang et al., 2021). It is necessary to strengthen VOC control and promote coordinated emission reduction of $PM_{2.5}$ and O_3. In Urumqi, a megacity located in western China, the levels of PM_{10} significantly decrease by 35.6%, and meteorological impacts dominated the declines. Some studies in other countries and regions also reveal the important role of meteorological conditions in air quality changes. A study of Israel showed that the total percentage change of pollution emissions explained by the lockdown was up to 26%, which increased to 47% by taking meteorological conditions as a factor in addition to the lockdown effect (Agami and Dayan, 2021). In India, Mandal et al. (2022) noted that adverse meteorological conditions exacerbated Delhi's air pollution situation.

3.4.2. True effects on air quality

Through a simple comparison before and after the lockdown, the concentration of pollutants is affected by meteorological conditions as well as seasonal changes in emissions (Hernandez-Paniagua et al., 2021). As shown in Fig. 7 (a), whether there is a lockdown or not, obvious changes in deweathered pollutants during the same periods were also observed in 2015–2019. For example, during the same period from 2015 to 2019, despite the absence of lockdown, deweathered O_3 increased 46.0%, 41.7%, and 52.9% (trend) in Wuhan, Beijing, and Urumqi, respectively (Table 3). In addition to the elimination of meteorological effects, the elimination of trends in "activity as usual" change is also crucial for estimating the actual change resulting from the intervention (i.e., the lockdown). In this section, our study quantified the true influence of regulatory behavior on air quality during the COVID-19 epidemics.

Considering urban stations in Beijing as an example, observed NO_2, $PM_{2.5}$, and O_3 changed by −42.9%, +21.7% and +76.4%, respectively (obtained from unadjusted concentration data before/during lockdown, Table 3). However, the observed values are considerably higher (sometimes by a factor of 10) than our detrended results, which are −19.8% for NO_2, -17.0% for $PM_{2.5}$ and +2.1% for O_3. This may demonstrate the necessity of disentangling the changes due to meteorological variation and seasonality and from the lockdown-driven changes in emissions to understand the resulting differences in air pollutant concentrations.

From Table 3 and S4, in Wuhan, the net effect due to lockdown was −17.3% (PM_{10}), −14.6% ($PM_{2.5}$), −3.6% (CO), −33.2% (NO_2) and +69.3% (O_3), respectively. In Beijing, the pollutant concentrations decreased by 17% ($PM_{2.5}$), 12.2% (CO), and 19.8% (NO_2). In Urumqi, the concentrations declined by 8.7% (PM_{10}), 34.0% ($PM_{2.5}$), 16.7% (CO) and 31.8% (NO_2). Our detrended results demonstrate that the decline in CAPs concentrations attributable to the lockdowns was not as large as that observed.

The true NO_2 decreased by 33.2%, 19.8%, and 31.8% in Wuhan, Beijing, and Urumqi, respectively. We investigated the change in the travel intensity in three cities during the study period (Fig. S7). Before the lockdown, the travel intensity in 2019 and 2020 was similar, while when the lockdown went into effect in 2020, the travel intensity decreased significantly compared with the same period last year. The travel intensity was reduced by 60.2%, 76.9%, and 86.3% in Beijing, Urumqi, and Wuhan (Fig. S7) during the lockdown period (2020.2.1–3.15) compared with pre-lockdown (2020.1.1–1.20). The travel intensity data refers to the exponential results of the ratio of the number of people who travel out of the city to the resident population in the city and can be used to measure the degree of urban vitality recovery (Wang et al., 2021). The change in the travel intensity index of the three cities is consistent with the decrease in NO_2. There is a strong correlation between NO_2 pollution and traffic activity intensity (Wang et al., 2021). Results in Table S2 show that the NO_2 level in three cities almost reached the National level standard (40 μg/m^3) due to the lockdown measures. According to our research, we found that traffic activity management is

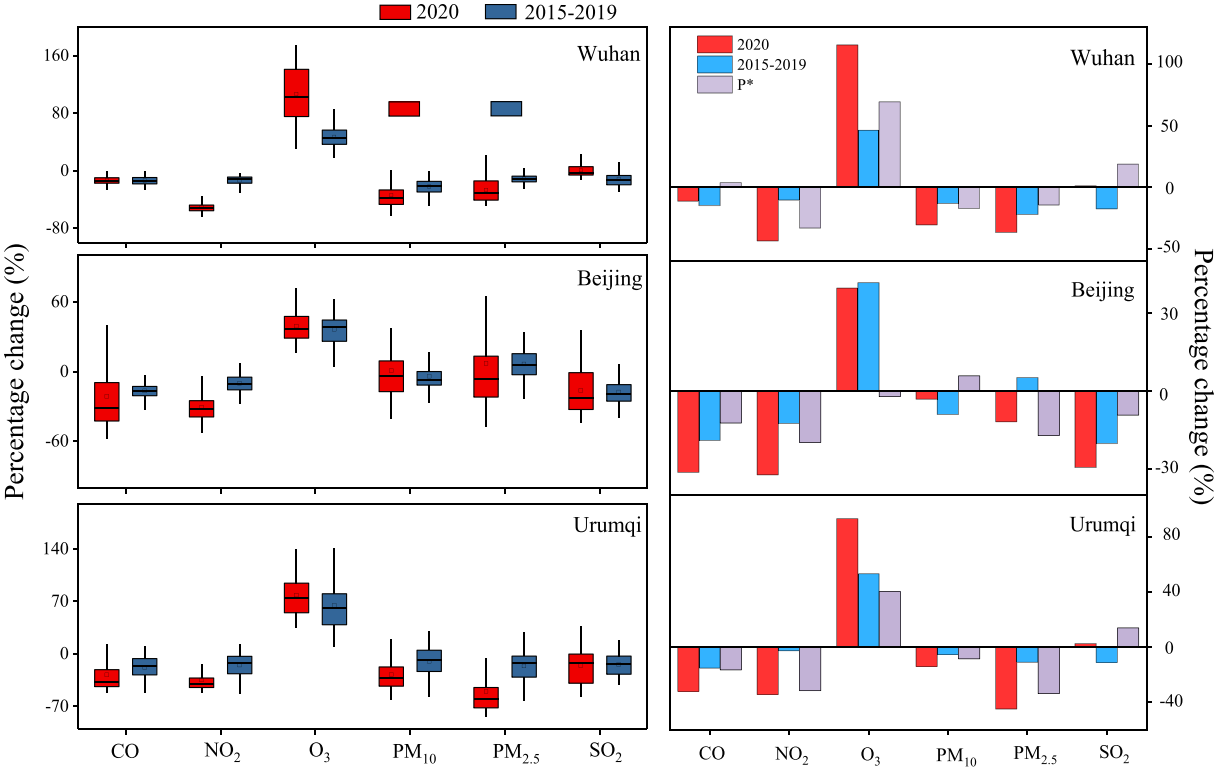


Fig. 7. (a) Concentration change rate of deweathered pollutants during lockdown period versus pre-lockdown period in 2020 and 2015–2019 and (b) the true percentage change (due to lockdown) of air pollutants at urban stations in three cities.

Table 3
Contribution of the three major driving factors to the decreasing trend of air pollutants in 2020 in Wuhan, Beijing, and Urumqi.

Cities		NO_2	O_3	$PM_{2.5}$	PM_{10}	CO	SO_2
Wuhan	△P	−49.7%	+145.4%	−36.7%	−33.7%	−12.5%	+12.5%
	Meteorological	−6.0%	+30.1%	+0.2%	−3.2%	−1.0%	+11.5%
	Trend	−10.5%	+46.0%	−22.3%	−13.2%	−15.1%	−17.5%
	COVID-19	−33.2%	+69.3%	−14.6%	−17.3%	+3.6%	+18.5%
Beijing	△P	−42.9%	+76.4%	+21.7%	−5.8%	−13.5%	−36.1%
	Meteorological	−10.6%	+36.8%	+33.5%	−2.8%	+17.7%	−6.8%
	Trend	−12.5%	+37.5%	+5.2%	−9.0%	−19.0%	−20.2%
	COVID-19	−19.8%	+2.1%	−17.0%	+6.0%	−12.2%	−9.1%
Urumqi	△P	−48.1%	+243.0%	−45.6%	−35.6%	−40.4%	+10.4%
	Meteorological	−13.3%	+150.0%	−0.4%	−21.1%	−8.1%	+8.1%
	Trend	−3.0%	+52.9%	−11.3%	−5.8%	−15.6%	−11.4%
	COVID-19	−31.8%	+40.1%	−33.9%	−8.7%	−16.7%	+13.7%

of great significance for NO_2 pollution control in densely populated urban areas.

4. Conclusions

In this study, we utilize a deweathering machine learning algorithm to explore the air quality variations caused by COVID-19 in three Chinese megacities at multiple scales and high resolutions. In terms of the overall tendency of air quality, the air quality in China's three megacities (Wuhan, Beijing, and Urumqi) improved due to the COVID-19 pandemic. However, the CAPs were found to have markedly different responses to containment measures at different stations in different cities. Our results emphasize the need for high spatial resolution ground-based research to capture the variation of different pollutants. From our results, NO_2 was the most sensitive to the lockdown in all three cities, deweathered NO_2 decreased by 43.7% in Wuhan, 34.8% in Urumqi and 32.2% in Beijing, a consequence of the decline in traffic activities. In Wuhan and Urumqi, deweathered CO and NO_2 decreased the most at traffic stations and the least at industry stations. However, unlike observations in Wuhan and Urumqi, deweathered NO_2 in Beijing showed the smallest decline at traffic stations (−24.8%). Although an increase in deweathered O_3 was generally observed, the increase was minimal at rural stations among three cities. In addition, the SO_2 variation reveals a mixed pattern, determined by city and station type. Removing the effects of meteorology, deweathered $PM_{2.5}$ declined by 36.9%, 11.8%, and 45.3% in Wuhan, Beijing, and Urumqi, respectively, which showed that reducing primary emissions from mobile sources is the most effective way to alleviate $PM_{2.5}$ pollution in Urumqi compared with Beijing and Wuhan. At the same time, we can see that the adverse meteorological conditions have a great effect on the occurrence of haze in Beijing. Consequently, it is essential to assess variations in air pollutant concentrations without meteorological influence.

After detrended analysis, we found that the lockdown did have a significant impact on air quality. The results show that the true percent change in CO, NO_2, and $PM_{2.5}$ ranged from −0.7% to −16.7%, −15.2% to −46.2%, and −2.3% to −40.2%, respectively. Reducing traffic activity is the most effective way to reduce NO_2 pollution. Although the largest percentage decrease in $PM_{2.5}$ was observed in Urumqi, its absolute concentration was still the highest among the three cities. This indicates that the situation of air pollution control in Urumqi is still very serious in the future. The optimization of the industrial structure and increase in clean energy use should be valued in Urumqi. In addition, the frequent pollution events that occurred during the lockdown suggest that actions on a similar scale are far from sufficient to prevent sporadic pollution events.

Our results show that there is obvious heterogeneity among different cities. Our study provides a reference for the change of pollutant concentration at the city scale during plugging. Future regulatory actions must adopt city-specific methods for NO_2, O_3, and $PM_{2.5}$, as well as several other non-criteria pollutants, such as VOCs and NH_3 which have not been under contiguously monitored at the current Chinese air quality monitoring stations, considering both primary discharge and secondary generation processes of pollutants to maximize the total benefits for air quality and human health.

CRediT author statement

Yunqian Lv: Conceptualization, Methodology, Modelling, Software, Investigation, Writing – original draft, preparation. **Hezhong Tian:** Conceptualization, Data curation, Formal analysis, Writing – review & editing, and, Supervision. **Lining Luo:** Validation, Formal analysis, Visualization. **Shuhan Liu:** Validation, Formal analysis, Visualization. **Xiaoxuan Bai:** Validation, Formal analysis, Visualization. **Hongyan Zhao:** Formal analysis, Writing – review & editing. **Shumin Lin:** Formal analysis, Visualization. **Shuang Zhao:** Formal analysis, Visualization. **Zhihui Guo:** Validation, Formal analysis. **Yifei Xiao:** Validation, Formal analysis. **Junqi Yang:** Validation, Formal analysis, All authors contributed to interpretation of the data and provided comments on the manuscript.

Declaration of competing interest

The authors declare that they have no known competing financial interests or personal relationships that could have appeared to influence the work reported in this paper.

Acknowledgements

This work was funded by the National Natural Science Foundation of China (22176014, 21777008), and the Trail Special Program of Research on the Cause and Control Technology of Air Pollution under the National Key Research and Development Plan of China (2019YFC0214201).

Appendix A. Supplementary data

Supplementary data to this article can be found online at https://doi.org/10.1016/j.apr.2022.101452.

References

Agami, S., Dayan, U., 2021. Impact of the first induced COVID-19 lockdown on air quality in Israel. Atmos. Environ. 262 https://doi.org/10.1016/j.atmosenv.2021.118627.

Bao, R., Zhang, A., 2020. Does lockdown reduce air pollution? Evidence from 44 cities in northern China. Sci. Total Environ. 731, 139052. https://doi.org/10.1016/j.scitotenv.2020.139052.

Breiman, L., 2001. Random forests. Mach. Learn. 45, 5–32. https://doi.org/10.1023/A:1010933404324.

Cameletti, M., 2020. The effect of corona virus lockdown on air pollution: evidence from the city of brescia in lombardia region (Italy). Atmos. Environ. 239 https://doi.org/10.1016/j.atmosenv.2020.117794.

Coccia, M., 2020. Factors determining the diffusion of COVID-19 and suggested strategy to prevent future accelerated viral infectivity similar to COVID. Sci. Total Environ. 729, 138474. https://doi.org/10.1016/j.scitotenv.2020.138474.

Cohen, A.J., Brauer, M., Burnett, R., Anderson, H.R., Frostad, J., Estep, K., Balakrishnan, K., Brunekreef, B., Dandona, L., Dandona, R., Feigin, V., Freedman, G., Hubbell, B., Jobling, A., Kan, H., Knibbs, L., Liu, Y., Martin, R., Morawska, L., Pope III, C.A., Shin, H., Straif, K., Shaddick, G., Thomas, M., van Dingenen, R., van Donkelaar, A., Vos, T., Murray, C.J.L., Forouzanfar, M.H., 2017. Estimates and 25-year trends of the global burden of disease attributable to ambient air pollution: an analysis of data from the Global Burden of Diseases Study 2015. Lancet 389 (10082), 1907–1918. https://doi.org/10.1016/s0140-6736(17)30505-6.

Cole, M.A., Elliott, R.J.R., Liu, B., 2020. The impact of the wuhan covid-19 lockdown on air pollution and health: a machine learning and augmented synthetic control approach. Environ. Resour. Econ. 76 (4), 553–580. https://doi.org/10.1007/s10640-020-00483-4.

Collivignarelli, M.C., Abba, A., Bertanza, G., Pedrazzani, R., Ricciardi, P., Miino, M.C., 2020. Lockdown for CoViD-2019 in Milan: what are the effects on air quality? Sci. Total Environ. 732, 139280. https://doi.org/10.1016/j.scitotenv.2020.139280.

Grange, S.K., Carslaw, D.C., 2019. Using meteorological normalisation to detect interventions in air quality time series. Sci. Total Environ. 653, 578–588. https://doi.org/10.1016/j.scitotenv.2018.10.344.

Guo, H., Kota, S.H., Sahu, S.K., Hu, J., Ying, Q., Gao, A., Zhang, H., 2017. Source apportionment of PM2. 5 in North India using source-oriented air quality models. Environ. Pollut. 231, 426–436. https://doi.org/10.1016/j.envpol.2017.08.016.

He, G., Pan, Y., Tanaka, T., 2020. The short-term impacts of COVID-19 lockdown on urban air pollution in China. Nat. Sustain. 3 (12) https://doi.org/10.1038/s41893-020-0581-y.

Hernandez-Paniagua, I.Y., Valdez, S.I., Almanza, V., Rivera-Cardenas, C., Grutter, M., Stremme, W., Garcia-Reynoso, A., Ruiz-Suarez, L.G., 2021. Impact of the COVID-19 lockdown on air quality and resulting public health benefits in the Mexico city metropolitan area. In: Frontiers in Public Health, vol. 9. https://doi.org/10.3389/fpubh.2021.642630.

Hu, Z., Wang, J., Chen, Y., Chen, Z., Xu, S., 2014. Concentrations and source apportionment of particulate matter in different functional areas of Shanghai, China. Atmos. Pollut. Res. 51, 138–144. https://doi.org/10.5094/apr.2014.017.

Huang, X., Ding, A., Gao, J., Zheng, B., Zhou, D., Qi, X., Tang, R., Wang, J., Ren, C., Nie, W., Chi, X., Xu, Z., Chen, L., Li, Y., Che, F., Pang, N., Wang, H., Tong, D., Qin, W., Cheng, W., Liu, W., Fu, Q., Liu, B., Chai, F., Davis, S.J., Zhang, Q., He, K., 2021. Enhanced secondary pollution offset reduction of primary emissions during COVID-19 lockdown in China. Natl. Sci. Rev. 8 (2), nwaa137. https://doi.org/10.1093/nsr/nwaa137.

Le, T., Wang, Y., Liu, L., Yang, J., Yung, Y.L., Li, G., Seinfeld, J.H., 2020. Unexpected air pollution with marked emission reductions during the COVID-19 outbreak in China. Science 369 (6504), 702. https://doi.org/10.1126/science.abb7431.

Lelieveld, J., Evans, J.S., Fnais, M., Giannadaki, D., Pozzer, A., 2015. The contribution of outdoor air pollution sources to premature mortality on a global scale. Nature 525 (7569), 367. https://doi.org/10.1038/nature15371.

Li, Q., Guan, X., Wu, P., Wang, X., Zhou, L., Tong, Y., Ren, R., Leung, K.S.M., Lau, E.H.Y., Wong, J.Y., Xing, X., Xiang, N., Wu, Y., Li, C., Chen, Q., Li, D., Liu, T., Zhao, J., Liu, M., Tu, W., Chen, C., Jin, L., Yang, R., Wang, Q., Zhou, S., Wang, R., Liu, H., Luo, Y., Liu, Y., Shao, G., Li, H., Tao, Z., Yang, Y., Deng, Z., Liu, B., Ma, Z., Zhang, Y., Shi, G., Lam, T.T.Y., Wu, J.T., Gao, G.F., Cowling, B.J., Yang, B., Leung, G.M., Feng, Z., 2020. Early transmission dynamics in wuhan, China, of novel coronavirus-infected pneumonia. N. Engl. J. Med. 382 (13), 1199–1207. https://doi.org/10.1056/NEJMoa2001316.

Liang, D., Shi, L., Zhao, J., Liu, P., Sarnat, J.A., Gao, S., Schwartz, J., Liu, Y., Ebelt, S.T., Scovronick, N., Chang, H.H., 2020. Urban air pollution may enhance COVID-19 case-fatality and mortality rates in the United States. Innovation 1 (3). https://doi.org/10.1016/j.xinn.2020.100047, 100047-100047.

Liu, F., Page, A., Strode, S.A., Yoshida, Y., Choi, S., Zheng, B., Lamsal, L.N., Li, C., Krotkov, N.A., Eskes, H., van der A, R., Veefkind, P., Levelt, P.F., Hauser, O.P., Joiner, J., 2020a. Abrupt decline in tropospheric nitrogen dioxide over China after the outbreak of COVID-19. Sci. Adv. 6 (28), eabc2992 https://doi.org/10.1126/sciadv.abc2992.

Liu, H., Wang, X.M., Pang, J.M., He, K.B., 2013. Feasibility and difficulties of China's new air quality standard compliance: PRD case of PM2.5 and ozone from 2010 to 2025. Atmos. Chem. Phys. 13 (23), 12013–12027. https://doi.org/10.5194/acp-13-12013-2013.

Liu, T., Wang, X., Hu, J., Wang, Q., An, J., Gong, K., Sun, J., Li, L., Qin, M., Li, J., Tian, J., Huang, Y., Liao, H., Zhou, M., Hu, Q., Yan, R., Wang, H., Huang, C., 2020b. Driving forces of changes in air quality during the COVID-19 lockdown period in the Yangtze River Delta region, China. Environ. Sci. Technol. Lett. 7 (11), 779–786. https://doi.org/10.1021/acs.estlett.0c00511.

Mahato, S., Pal, S., Ghosh, K.G., 2020. Effect of lockdown amid COVID-19 pandemic on air quality of the megacity Delhi, India. Sci. Total Environ. 730, 139086. https://doi.org/10.1016/j.scitotenv.2020.139086.

Mandal, J., Chanda, A., Samanta, S., 2022. Air pollution in three megacities of India during the Diwali festival amidst COVID-19 pandemic. Sustain. Cities Soc. 76, 103504. https://doi.org/10.1016/j.scs.2021.103504.

Murphy, J.G., Day, D.A., Cleary, P.A., Wooldridge, P.J., Millet, D.B., Goldstein, A.H., Cohen, R.C., 2007. The weekend effect within and downwind of Sacramento - Part 1: observations of ozone, nitrogen oxides, and VOC reactivity. Atmos. Chem. Phys. 7 (20), 5327–5339. https://doi.org/10.5194/acp-7-5327-2007.

Pei, Z., Han, G., Ma, X., Su, H., Gong, W., 2020. Response of major air pollutants to COVID-19 lockdowns in China. Sci. Total Environ. 743, 140879. https://doi.org/10.1016/j.scitotenv.2020.140879.

Petetin, H., Bowdalo, D., Soret, A., Guevara, M., Jorba, O., Serradell, K., Perez Garcia-Pando, C., 2020. Meteorology-normalized impact of the COVID-19 lockdown upon NO2 pollution in Spain. Atmos. Chem. Phys. 20 (18), 11119–11141. https://doi.org/10.5194/acp-20-11119-2020.

Rathod, A., Sahu, S.K., Singh, S., Beig, G., 2021. Anomalous behaviour of ozone under COVID-19 and explicit diagnosis of O-3-NOx-VOCs mechanism. Heliyon 7 (2). https://doi.org/10.1016/j.heliyon.2021.e06142.

Sharma, S., Zhang, M., Anshika Gao, J., Zhang, H., Kota, S.H., 2020. Effect of restricted emissions during COVID-19 on air quality in India. Sci. Total Environ. 728, 138878. https://doi.org/10.1016/j.scitotenv.2020.138878.

Sheng, T., Pan, J., Duan, Y., Liu, Q., Fu, Q., 2019. Study on characteristics of typical traffic environment air pollution in shanghai. China Environ. Sci. 39 (8), 3193–3200.

Shi, Z., Song, C., Liu, B., Lu, G., Xu, J., Tuan Van, V., Elliott, R.J.R., Li, W., Bloss, W.J., Harrison, R.M., 2021. Abrupt but smaller than expected changes in surface air quality attributable to COVID-19 lockdowns. Sci. Adv. 7 (3), eabd6696 https://doi.org/10.1126/sciadv.abd6696.

Sicard, P., De Marco, A., Agathokleous, E., Feng, Z., Xu, X., Paoletti, E., Dieguez Rodriguez, J.J., Calatayud, V., 2020. Amplified ozone pollution in cities during the COVID-19 lockdown. Sci. Total Environ. 735, 139542. https://doi.org/10.1016/j.scitotenv.2020.139542.

Singh, V., Singh, S., Biswal, A., Kesarkar, A.P., Mor, S., Ravindra, K., 2020. Diurnal and temporal changes in air pollution during COVID-19 strict lockdown over different regions of India. Environ. Pollut. 266, 115368. https://doi.org/10.1016/j.envpol.2020.115368.

Srivastava, A.K., Bhoyar, P.D., Kanawade, V.P., Devara, P.C.S., Thomas, A., Soni, V.K., 2021. Improved air quality during COVID-19 at an urban megacity over the Indo-Gangetic Basin: from stringent to relaxed lockdown phases. Urban Clim. 36, 100791. https://doi.org/10.1016/j.uclim.2021.100791.

Sun, Y., Lei, L., Zhou, W., Chen, C., He, Y., Sun, J., Li, Z., Xu, W., Wang, Q., Ji, D., Fu, P., Wang, Z., Worsnop, D.R., 2020. A chemical cocktail during the COVID-19 outbreak in Beijing, China: insights from six-year aerosol particle composition measurements during the Chinese New Year holiday. Sci. Total Environ. 742, 140739. https://doi.org/10.1016/j.scitotenv.2020.140739.

Tian, H., Liu, Y., Li, Y., Wu, C.-H., Chen, B., Kraemer, M.U.G., Li, B., Cai, J., Xu, B., Yang, Q., Wang, B., Yang, P., Cui, Y., Song, Y., Zheng, P., Wang, Q., Bjornstad, O.N., Yang, R., Grenfell, B.T., Pybus, O.G., Dye, C., 2020. An investigation of transmission control measures during the first 50 days of the COVID-19 epidemic in China. Science 368 (6491), 638. https://doi.org/10.1126/science.abb6105.

Venter, Z.S., Aunan, K., Chowdhury, S., Lelieveld, J., 2020. COVID-19 lockdowns cause global air pollution declines. Proc. Natl. Acad. Sci. U.S.A. 117 (32), 18984–18990. https://doi.org/10.1073/pnas.2006853117.

Vu, T.V., Shi, Z., Cheng, J., Zhang, Q., He, K., Wang, S., Harrison, R.M., 2019. Assessing the impact of clean air action on air quality trends in Beijing using a machine learning technique. Atmos. Chem. Phys. 19 (17), 11303–11314. https://doi.org/10.5194/acp-19-11303-2019.

Wang, J., Xu, X., Wang, S., He, S., He, P., 2021. Heterogeneous effects of COVID-19 lockdown measures on air quality in Northern China. Appl. Energy 282, 116179. https://doi.org/10.1016/j.apenergy.2020.116179.

Wang, P., Chen, K., Zhu, S., Wang, P., Zhang, H., 2020. Severe air pollution events not avoided by reduced anthropogenic activities during COVID-19 outbreak. Resour. Conserv. Recycl. 158, 104814. https://doi.org/10.1016/j.resconrec.2020.104814.

Wang, Y., Wen, Y., Wang, Y., Zhang, S., Zhang, K.M., Zheng, H., Xing, J., Wu, Y., Hao, J., 2020. Four-month changes in air quality during and after the COVID-19 lockdown in six megacities in China. Environ. Sci. Technol. Lett. 711, 802–808. https://doi.org/10.1021/acs.estlett.0c00605.

Wu, C., Wang, H., Cai, W., He, H., Ni, A., Peng, Z., 2021. Impact of the COVID-19 Lockdown on Roadside Traffic-Related Air Pollution in Shanghai, China. Building and Environment, p. 194. https://doi.org/10.1016/j.buildenv.2021.107718.

Xue, Y., Zhang, S., Zhou, Z., Wang, K., Liu, K., Wang, X., Shi, A., Xu, K., Tian, H., 2019. Spatio-temporal variations of multiple primary air pollutants emissions in beijing of China, 2006-2015. Atmosphere 10 (9), 494. https://doi.org/10.3390/atmos10090494.

Zhang, Q., Zheng, Y., Tong, D., Shao, M., Wang, S., Zhang, Y., Xu, X., Wang, J., He, H., Liu, W., Ding, Y., Lei, Y., Li, J., Wang, Z., Zhang, X., Wang, Y., Cheng, J., Liu, Y., Shi, Q., Yan, L., Geng, G., Hong, C., Li, M., Liu, F., Zheng, B., Cao, J., Ding, A., Gao, J., Fu, Q., Huo, J., Liu, B., Liu, Z., Yang, F., He, K., Hao, J., 2019. Drivers of improved PM2.5 air quality in China from 2013 to 2017. Proc. Natl. Acad. Sci. U.S.A. 116 (49), 24463–24469. https://doi.org/10.1073/pnas.1907956116.

Zhao, X., Wang, G., Wang, S., Zhao, N., Zhang, M., Yue, W., 2021. Impacts of COVID-19 on air quality in mid-eastern China: an insight into meteorology and emissions. Atmos. Environ. 266 https://doi.org/10.1016/j.atmosenv.2021.118750.

Zhang, Y., Vu, V., Sun, J., He, J., Shen, X., Lin, W., Zhang, X., Zhong, J., Gao, W., Wang, Y., Fu, T., Ma, Y., Li, W., Shi, Z., 2020. Significant changes in chemistry of fine particles in wintertime beijing from 2007 to 2017: impact of clean air actions. Environ. Sci. Technol. 54 (3), 1344–1352. https://doi.org/10.1021/acs.est.9b04678.